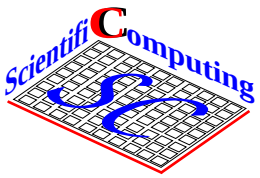


# Efficient Model Reduction in Non-linear Dynamics Using the Karhunen-Loève Expansion and Dual-Weighted-Residual Methods

Marcus Meyer, Hermann G. Matthies
Institute of Scientific Computing
Technical University Braunschweig
Brunswick, Germany

Informatikbericht Nr.: 2003-01

December 2002

# Efficient Model Reduction in Non-linear Dynamics Using the Karhunen-Loève Expansion and Dual-Weighted-Residual Methods

Marcus Meyer, Hermann G. Matthies
Department of Computer Science
Technical University Braunschweig
Brunswick, Germany

Informatikbericht Nr.: 2003-01

December 2002

Contributed to a Special Issue of *Computational Mechanics*

**Location**
Institute of Scientific Computing
Technische Universität Braunschweig
Hans-Sommer-Strasse 65
D-38106 Braunschweig

**Postal Address**
Institut für Wissenschaftliches Rechnen
Technische Universtität Braunschweig
D-38092 Braunschweig
Germany

**Contact**
Phone: +49-(0)531-391-3000
Fax: +49-(0)531-391-3003
E–Mail: wire@tu-bs.de

# Efficient Model Reduction in Non-linear Dynamics Using the Karhunen-Loève Expansion and Dual-Weighted-Residual Methods

Marcus Meyer Hermann G. Matthies
Institute of Scientific Computing
Technical University of Braunschweig
Brunswick, Germany
December 2002

**Abstract**

We look at the task of computing the time-evolution of a non-linear system for a long time, in our case under random external influences. Our specific example is the fatigue evaluation of a wind turbine. To facilitate such a computation, we look at a reduction of the computational effort by projecting everything on a low-dimensional basis. In this case we take the Karhunen-Loève basis generated from running the model a little while under the random loading. It is important that we error which is caused by this reduction process can be controlled. We estimate the error by dual or adjoint methods. This in turn allows the process of model reduction to be performed adaptively.

**Keywords:** model reduction, non-linear dynamics, Karhunen-Loève expansion, error estimates, dual-weighted-residual-methods

# Contents

# 1 Introduction

Although computing speed still increases significantly from year to year, the analysis of non-linear instationary problems can still be a computationally intensive task. This is especially the case when many of calculations have to be performed, for example when optimising the dynamic behaviour or analysing the fatigue loading of wind turbines: In this application a large number of long-time integrations have to be calculated for different wind speeds and operating conditions, and decreasing the computing time of the individual simulation is of great importance.

The solution process in the field of structural dynamics normaly proceeds as follows, compare Fig. 1: The non-linear partial differential equations describing the system of interest are discretised in space using the finite element method. To obtain a good approximation quality, one typically uses a fine discretisation, resulting in a large number of nodal unkowns. This leads to a very large system of non-linear ordinary differential equations with time as the remaining variable.

For the following discretisation in time we can use either explicit or implicit methods. Both methods have advantages and disadvantages: Using an explicit method we avoid the solution of a large system of non-linear algebraic equations in each time step, but the size of the time step is severly limited by stability considerations. Implicit methods allow larger time steps [50], but iteratively solving the non-linear system by repeated solutions of linear systems can be very time and memory consuming.

In both cases model reduction can significantly reduce the necessary amount of computation: In the case of explicit time integration high frequencies, which are present in the model only due to the fine spatial discretisation and do not have a physical meaning in most applications, can be eliminated and thus the stable time step length increased, see e.g. BUCHER [8]. When using implicit time integration, the model reduction drastically reduces the size of the repeatedly solved system of linear equations, as shown in KRYSL et al. [29] or REMKE and ROTHERT [43]. Also the non-physical high frequency content of the dynamic solution is eliminated.

The idea of projection-based model reduction lies in the transition from the original variables, in our case the large number of nodal variables of the finite element model, to a very small number of generalised variables, which only describe the large-scale structures dominating the system dynamics. This is accomplished by projecting the original system onto a low-dimensional subspace. Consider for example the vibration of a clamped beam, exited by a time-varying external force. The displacement field of the beam can be very efficiently (and with good approximation quality) described in the subspace spanned by only very few of the clamped beam's eigenmodes, whose eigenfrequencies lie in the vicinity of the frequencies present in the excitation. These large-scale structures are also present in

fluid dynamics, where they are called coherent structures [19], as example consider the eddies in the wake of a body.

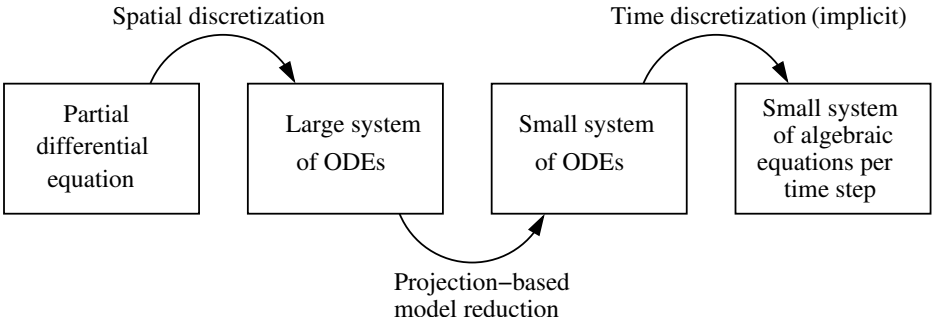


Figure 1: Solution process involving the model reduction step.

In the following we first describe the general procedure of projection-based model reduction. Then we describe different choices for the basis vectors, emphasising the Karhunen-Loève basis for non-linear dynamics. In the next section the approximation error of the reduced model compared to the full one is analysed employing the dual-weighted residual method. We also show how to use the error estimate to find a problem-specific efficient low-dimensional basis. The last section gives numerical examples from the analysis of the dynamic behaviour of flexible wind turbines showing the applicability of the proposed approach.

# 2 Projection-Based Model Reduction

Performing the spatial discretisation, we obtain a large system of non-linear ordinary differential equations of second order,

$$\boldsymbol{F}(\ddot{\boldsymbol{d}}, \dot{\boldsymbol{d}}, \boldsymbol{d}, t) = \boldsymbol{0}, \tag{1}$$

together with the initial conditions

$$\boldsymbol{d}(0) = \boldsymbol{d}_0, \quad \dot{\boldsymbol{d}}(0) = \boldsymbol{v}_0. \tag{2}$$

The dimension of this system is $n$, i.e. $\boldsymbol{d} \in \mathbb{R}^n$. To reduce the size of this system, we choose an ansatz of the form

$$\boldsymbol{d}(t) \approx \boldsymbol{d}_m(t) = \sum_{j=1}^{m} \boldsymbol{y}_j \xi_j(t) = \boldsymbol{Y}_m \boldsymbol{\xi}(t). \tag{3}$$

The matrix $\boldsymbol{Y}_m = [\boldsymbol{y}_1, \ldots, \boldsymbol{y}_m]$ is formed by $m$ vectors $\boldsymbol{y}_i$, arranged column-wise. These vectors have to be linearly independent, so that they span a subspace $\mathcal{Y}_m$ of dimension $m$ of the original $d$-dimensional space, $\boldsymbol{\xi} \in \mathbb{R}^m$, $\mathcal{Y}_m = \text{span}\{\boldsymbol{y}_1, \ldots, \boldsymbol{y}_m\}$. This subspace is called the ansatz space. As the model reduction leads from a system of size $n$ to a system of size $m$, $1 < m \ll n$ is desirable.

Next we need the space of test functions $\hat{\mathcal{Y}}_m = \text{span}\{\hat{\boldsymbol{y}}_1, \ldots, \hat{\boldsymbol{y}}_m\}$. Here we have two choices: The Bubnov-Galerkin method sets $\mathcal{Y}_m = \hat{\mathcal{Y}}_m$, the Petrov-Galerkin method uses $\hat{\mathcal{Y}}_m \neq \mathcal{Y}_m$. In our computations we have used the choice $\boldsymbol{Y}_m = \hat{\boldsymbol{Y}}_m$.

If we substitute the approximation Eq.(3) for $\boldsymbol{d}$ and its derivatives in Eq.(1), we obtain a non-zero residual $\boldsymbol{\rho}$,

$$\boldsymbol{\rho} = \boldsymbol{F}(\boldsymbol{Y}_m\ddot{\boldsymbol{\xi}}, \boldsymbol{Y}_m\dot{\boldsymbol{\xi}}, \boldsymbol{Y}_m\boldsymbol{\xi}, t). \tag{4}$$

In the last step of the reduction process we require this residual to be orthogonal to the test space $\mathcal{Y}_m$, by multiplying the equation with $\boldsymbol{Y}_m^T$ from the left and setting it to zero:

$$\boldsymbol{Y}_m^T\,\boldsymbol{\rho} = \boldsymbol{0}. \tag{5}$$

Compared to the true solution $\boldsymbol{d}$, the approximate solution $\boldsymbol{d}_m$ has an error

$$\boldsymbol{e} = \boldsymbol{d} - \boldsymbol{d}_m. \tag{6}$$

This error $\boldsymbol{e}$ is orthogonal to the test space $\mathcal{Y}_m$, and is due to the fact that only that part $\boldsymbol{d}_m$ of the solution $\boldsymbol{d}$ is calculated which lies in the choosen subspace. This is the "Galerkin orthogonality condition". Before we describe a method to estimate this error $\boldsymbol{e}$ in section 3, we take a closer look at the columns in the matrix $\boldsymbol{Y}_m$, the basis vectors of the low-dimensional subspace.

## 2.1 Choosing the Basis

The approximation quality of the reduced model depends highly on the choice of the basis vectors. The best choice from the numerical point of view is an orthogonal basis for both test and ansatz space, see e.g. [12]. In the literature one can find many different proposals for the choice of the reduced basis in structural dynamics applications, cf. DINKLER [10], NOOR [38], as well as LEGER and DUSSAULT [30] for an overview.

Concerning linear structural dynamics the use of eigenmodes is well established. This is called modal reduction and leads to a separation of variables. A second advantage is the physical meaning of the eigenmodes, leading to criteria

to select the important eigenmodes, based for example on the comparison of frequency content of the loading with eigenfrequencies of the modes. The first who used the concept of eigenmodes for the model reduction of non-linear systems was NICKELL [37]. At the beginning of each time step he forms the linearised system to obtain a new set of eigenmodes for the following time step via the generalised eigenvalue problem

$$\boldsymbol{K}\boldsymbol{y} = \lambda^2 \boldsymbol{M}\boldsymbol{y} \tag{7}$$

for the eigenvectors $\boldsymbol{y}_i$ and eigenvalues $\lambda_i^2$. $\boldsymbol{M}$ is the tangent mass matrix and $\boldsymbol{K}$ the tangent stiffness matrix at the known initial condition $\boldsymbol{d}_0$ for the following time step,

$$\boldsymbol{M} = \left.\frac{\partial \boldsymbol{F}}{\partial \ddot{\boldsymbol{d}}}\right|_{\boldsymbol{d}_0}, \quad \boldsymbol{K} = \left.\frac{\partial \boldsymbol{F}}{\partial \boldsymbol{d}}\right|_{\boldsymbol{d}_0}. \tag{8}$$

The repeated solution of this eigenvalue problem is computationally intensive. Also IDELSON and CARDONA [21] show that frequent changes of the basis equals the introduction of a time dependent constraint, which can change the dynamic behaviour of the model and even lead to numerical stability problems. The reason lies in the necessity to repeatedly project the "old" velocities and accelerations in the "new" subspace. Therefore, if the non-linearity of the system is weak or moderate, it is best to use the eigenvectors of the linearisation at the initial condition for the whole computation.

A second, often-cited choice for the basis employs the Krylov subspace, see for example NOUR-OMID and CLOUGH [40], or WILSON et al. [49]. Here an orthogonal basis spanning the Krylov subspace $\mathcal{K}_m$ of dimension $m$,

$$\mathcal{K}_m = \text{span}\{\boldsymbol{y}_1, \boldsymbol{A}\boldsymbol{y}_1, \boldsymbol{A}^2\boldsymbol{y}_1, \ldots \boldsymbol{A}^{m-1}\boldsymbol{y}_1\}, \tag{9}$$

is calculated using the Arnoldi or Lanczos algorithm, cf. [44] for details.

In structural dynamics the matrix $\boldsymbol{A}$ is often choosen to equal $\boldsymbol{A} = \boldsymbol{K}^{-1}\boldsymbol{M}$, which is symmetric in the $\boldsymbol{M}$ inner product, and the start vector $\boldsymbol{y}_1$ is taken to be the solution of the linear static problem $\boldsymbol{K}\boldsymbol{d} = \boldsymbol{f}$ with a "representative" load $\boldsymbol{f}$. Note that again the linearisation of the non-linear problem is necessary to calculate this basis. Compared to the modal basis the advantage of the Lanczos basis lies in the fact that no eigenvalue problem has to be solved. Secondly this method includes the spatial distribution of the representative loading and often leads to a better approximation of secondary variables like inner forces and moments.

Apart from the modal and Lanczos basis a survey of the literature also yields "mixed" bases with additional ingredients: ALMROTH et al. [1] use the displacement increment of the first iteration in the Newton-Raphson procedure as additional vector in the reduced basis, NOOR and PETERS [39] employ derivatives of

the solution trajectory as additional generalised coordinates, NOOR [38] proposes a mixture of eigenmodes and Lanczos vectors and IDELSON and CARDONA [21] use tangent eigenmodes together with their approximated time derivatives.

## 2.2 The Karhunen-Loève Basis

Quite recent is the use of the Karhunen-Loève (KL) expansion [25, 34] for non-linear structural dynamics, already employed by KREUZER and KUST [28], KRYSL et al. [29] and SANSOUR [45]. This basis disguises itself under a large number of different names in the literature: Principal components [20], empirical orthogonal eigenvectors [33], factor-analysis [18], proper orthogonal decomposition [35] and total least squares [16], further informations can be found in HOLMES et al. [19] or SIROVITCH and EVERSON [47].

The idea of the KL-expansion is based on an optimality argument: Given a number of realisations $\{q^k(x)\}$ of a scalar field $q(x)$, defined on the set $Q$ in the Hilbert space $L_2(Q)$, find that basis $\{y_j(x)\}_{j=1}^m$, which is optimal in the sense that the $m$-dimensional approximation

$$q_m(x) = \sum_{j=1}^{m} \xi_j y_j(x) \tag{10}$$

describes a typical member of the ensemble $\{q^k\}$ better than the use of *any* other $m$-dimensional basis. In other words: Choose the basis functions $y$ to maximise the mean projection of the function $q$ on $y$,

$$\max_{y \in L_2(Q)} \frac{E(|\langle q, y\rangle|^2)}{\|y\|^2}. \tag{11}$$

with $E\{\bullet\}$ denoting the expectation or mean value functional. HOLMES [19] then shows that the basis functions are solutions of the following Fredholm integral equation,

$$\int_Q E(q(x_1)q(x_2))y(x_2)dx_2 = \lambda y(x_1), \tag{12}$$

whose kernel $G(x_1, x_2) = E(q(x_1)q(x_2))$ is the auto-covariance function of the two points $x_1$ and $x_2$. This kernel is by definition symmetric and positive definite, and, if $G$ is regular enough, defines a compact operator on $L_2(Q)$, hence has real and non-negative eigenvalues with only possible accumulation point zero. In the finite-dimensional case, where the ensemble members $\{\boldsymbol{q}^k\}$ are vectors in $\mathbb{R}^n$, we get a simple geometric interpretation of the optimal basis: The auto-covariance function is replaced by the matrix

$$\boldsymbol{G}_{jk} = E(\boldsymbol{q^j} \otimes \boldsymbol{q^k}), \tag{13}$$

and the eigenvectors of this matrix are the principal components of the cloud of data points $\{\boldsymbol{q}^k\}$ in the space $\mathbb{R}^n$.

We apply this approach to the low-dimensional description of structural dynamics. As example we take the function $q(x,t),\ x \in [0,L],\ \ t \in [0,T]$, for the sake of simplicity defined on a one-dimensional domain in space and time. This function describes the deviation of the displacement of a structure from the temporal mean. We assume that $q(x,t)$ is continuous with time-averaged autocovariance function $G(x,x^*)$. Using the eigenfunctions $\{y_j\}$ and eigenvalues $\lambda_j$ of the integral operator with kernel $G$,

$$\int_0^L G(x_1,x_2)y_j(x_2)dx_2 = \lambda_j y_j(x_1), \tag{14}$$

we can write $q(x,t)$ as

$$q(x,t) = \sum_{j=1}^{\infty} \sqrt{\lambda_j}\ \xi_j(t)\ y_j(x). \tag{15}$$

Here the functions $\xi_j(t)$ satisfy the equation

$$\xi_j(t) = (\sqrt{\lambda_j})^{-1} \int_0^L y_j(x)q(x,t)dx \tag{16}$$

and are uncorrelated, $E(\xi_n\xi_m) = \delta_{nm}$.

### 2.2.1 Optimalitity of the Karhunen-Loève Expansion

Before we continue with the calculation of the basis functions, we would like to quickly comment on the optimality of the KL basis: We can interpret the eigenvalues $\lambda_j$ as the mean energy of the displacement, projected on the eigenfunction $y_j$, since if we define the mean energy-projection to be $E(|\langle y_j, q\rangle|^2)$, we obtain (the averaging is now to be understood as an average over time):

$$E\left(|\langle y_j, q\rangle|^2\right) = E\left(\left|\int_0^L y_j(x)q(x,t)dx\right|^2\right) = \lambda_j. \tag{17}$$

Ordering the eigenvalues $\lambda_j$ in descending order, $\lambda_j > \lambda_{j+1}\ \forall\ j$, we obtain the relation (cf. [7]),

$$\sum_{j=1}^{m} E(|\langle y_j, q(x,t)\rangle|^2) = \sum_{j=1}^{m} \lambda_j\ \geq\ \sum_{j=1}^{m} E(|\langle z_j, q(x,t)\rangle|^2) \tag{18}$$

for any choice of $m$ and other basis functions $z_j$. This means that of all linear decompositions of the function $q(x,t)$ for a given number $m$ of basis vectors, the Karhunen-Loève expansion is the most efficient in the sense that the projection of $q(x,t)$ on the subspace spanned by $y_j$ contains the maximal amount of energy.

We can also define optimalitity as the search for those basis functions, that minimise the norm of the difference between exact solution and approximation,

$$E \quad (\|q(x,t) - \sum_{j=1}^{m} \xi_j y_j\|^2) =$$

$$E \quad (\|q(x,t)\|^2) + E(\|\sum_{j=1}^{m} \xi_j y_j\|^2) - 2E(\langle q(x,t), \sum_{j=1}^{m} \xi_j y_j \rangle).$$

This leads to maximising the sum of the projections $\sum_{j=1}^{N} E(\langle q, y_j \rangle)$, which is exactly the idea on which the Karhunen-Loève expansion is based, as explained in the introduction.

### 2.2.2 The Method of Snapshots

To actually calculate the Karhunen-Loève basis, we have to solve a large eigenvalue problem, even if the spatial discretisation is only moderatly fine. An approach to reduce the amount of computational work has been formulated by SIROVITCH [46] and is called the "method of snapshots". Suppose that a simulation or an experiment has provided a displacement field $q(x,t)$. With $q(x, n\Delta t) = q_n(x)$ we describe a number $M$ of discrete snapshots of the displacement field with constant time step $\Delta t$. Employing the assumption of ergodicity, the spatial covariance function can be written as

$$G(x_1, x_2) = \lim_{T \to \infty} \frac{1}{T} \int_0^T q(x_1, t) q(x_2, t) dt. \tag{19}$$

To approximate this equation we use the snapshots,

$$\hat{G}_M(x_1, x_2) = \frac{1}{M} \sum_{k=1}^{M} q_k(x_1, t_k) q_k(x_2, t_k). \tag{20}$$

The function $\hat{G}_M(x_1, x_2)$ is called the empirical spatial covariance function. To calcualte the KL basis vectors one needs the integral operator with kernel

$G(x_1, x_2)$,

$$\int_0^L G(x_1,x_2)y(x_2)dx_2 \approx \int_0^L \frac{1}{M}\sum_{k=1}^{M} q_k(x_1)q_k(x_2)y(x_2)dx_2 \tag{21}$$

$$= \frac{1}{M}\sum_{k=1}^{M} q_k(x_1)\int_0^L q_k(x_2)y(x_2)dx_2 \tag{22}$$

$$= \sum_{k=1}^{M}\alpha_k q_k(x_1). \tag{23}$$

The eigenfunctions $y(x)$ of the integral operator must satisfy

$$\sum_{k=1}^{M}\alpha_k q_k(x) = \lambda\, y(x). \tag{24}$$

This means we can write the empirical eigenfunctions as

$$y(x) = \sum_{k=1}^{M}\beta_k q_k(x) = \boldsymbol{\beta}^T\boldsymbol{q}(x) \tag{25}$$

with the constants $\boldsymbol{\beta} = (\beta_1, \ldots, \beta_M)^T$ and the vector of snapshots $\boldsymbol{q}(x) = (q_1(x), \ldots, q_M(x))^T$. Thus we obtainthat the empirical eigenfunctions of the integral operator with the kernel $\hat{G}_M(x_1, x_2)$ are linear combinations of the snapshots of the displacement field.

Let us return to the calculation of the empirical eigenfunctions, i.e. to the solution of

$$\int_0^L G(x_1,x_2)y(x_2)dx_2 = \lambda\, y(x_1). \tag{26}$$

Here we substitute the empirical spatial covariance functions and also Eq.(25) and obtain

$$\int_0^L \frac{1}{M}\sum_{k=1}^{M} q_k(x_1)q_k(x_2)\sum_{m=1}^{M}\beta_m q_m(x_2)dx_2 = \lambda\sum_{k=1}^{M}\beta_k q_k(x_1) = \tag{27}$$

$$\frac{1}{M}\sum_{k=1}^{M} q_k(x_1)\sum_{m=1}^{M}\beta_m\int_0^L q_k(x_2)q_m(x_2)dx_2 = \lambda\sum_{k=1}^{M}\beta_k q_k(x_1). \tag{28}$$

This we can write as

$$(\boldsymbol{B}\boldsymbol{\beta})^T\boldsymbol{q}(x) = \lambda\boldsymbol{\beta}^T\boldsymbol{q}(x), \tag{29}$$

with the elements of the matrix $\boldsymbol{B}$ defined as

$$B_{ij} = \frac{1}{M} \int_0^L q_i(x) q_j(x) dx. \tag{30}$$

With the assumption that the snapshots are linearly independent, i.e. that the matrix $\boldsymbol{B}$ is positive definite, we can deduce from

$$(\boldsymbol{B}\boldsymbol{\beta})^T \boldsymbol{q}(x) = \lambda \boldsymbol{\beta}^T \boldsymbol{q}(x), \tag{31}$$

that also

$$\boldsymbol{B}\boldsymbol{\beta} = \lambda \boldsymbol{\beta} \tag{32}$$

holds true. This leads to the final result that the unkown constants in Eq.(25) are given by the eigenvectors of Eq.(32). Since this eigenvalue problem has only the dimension $M$ and not on the dimension $n$ of the discretised system, the computational work is reduced significantly.

To summerise, we give the "recipe" to calculate the KL basis: Solve the non-linear system for a certain amount of time. Save the discretised snapshots $\boldsymbol{d}_i$ and calculate their temporal mean $\bar{\boldsymbol{d}} = \frac{1}{M} \sum_{i=1}^{M} \boldsymbol{d}_i$. Form the matrix $\boldsymbol{D} = [\boldsymbol{d}_1 - \bar{\boldsymbol{d}}, \ldots, \boldsymbol{d}_M - \bar{\boldsymbol{d}}]$. Then calculate matrix $\boldsymbol{B}$,

$$\boldsymbol{B} = \frac{1}{M} \boldsymbol{D}^T \boldsymbol{D}. \tag{33}$$

Using the eigenvectors $\boldsymbol{\beta}_j$ of this matrix,

$$\boldsymbol{B}\boldsymbol{\beta}_j = \lambda_j \boldsymbol{\beta}_j, \tag{34}$$

the KL basis vectors are given by

$$\boldsymbol{y}_j = \boldsymbol{D}\boldsymbol{\beta}_j. \tag{35}$$

Note that no linearisation is necessary to obtain the basis, but instead one has to solve the unreduced non-linear system for a certain amount of time.

# 3 Error Estimation and Adaptivity

It is important to analyse the error of the approximate compared to the exact solution to be able to judge the quality of the reduced model. For linear structural systems one can find some approaches in the literature: KLINE [27] analyses the error of models which have been reduced using a combination of modal and Lanczos basis. He shows that the error consists of two parts: The first part is due to the

lack of the reduced basis to fully represent the external force, the second part of the error comes through the inability of the reduced model to reproduce the exact vibration response of the unreduced system. JOO, WILSON and LEGER [24] give criteria for the necessary dimension of the Lanczos basis, based on the analysis of the model reduction error. They show that those components of the external force, which are orthogonal to the reduced basis, contribute significantly to the error. CABOS [9] calculates a-posteriori error bounds for linear vibration problems, which are approximated in the Krylov subspace. He derives a bound for the norm of the unkown error and also a bound for the error of a functional of the solution.

For non-linear systems little work on error estimation of the reduced model can be found in the literature: FINK and RHEINBOLDT [15, 14] give an estimation of the error of reduced non-linear static problems and derive, that this error decreases with increasing dimension of the reduced basis. UTKU et al. [48] give estimates for the model reduction error for non-linear systems of first order, which are discretised with the expicit Euler method in time. The result is an approximation of the error in every time step, which include the unkown exact solution.

## 3.1 The Dual-Weighted-Residual Method

In the following we want to describe a novel technique for calculating the model reduction error of non-linear systems: The dual-weighted-residual (DWR) method uses the solution of a dual or adjoint system to obtain an estimate of the error. In the field of parameter sensitivity analysis and optimisation this method is well known and established [3, 22, 26]. But also for the estimation of the discetisation error of partial differential equations in space and time and for adaptive mesh refinement this approach has been used with good success, see for example JOHNSON [23] and ERIKSSON et al. [11], as well as the work of RANNACHER et al. [42, 5, 4, 2, 6] and ESTEP and LOGG [13, 32, 31]. Further information can be found in RANNACHER [41], for a thorough treatment of the adjoint method see KLEIBER [26] and MARCHUK [36].

To introduce the concept of the DWR method, we first consider the linear static problem

$$\boldsymbol{K}\boldsymbol{d} = \boldsymbol{f}, \quad \boldsymbol{d} \in \mathbb{R}^n. \tag{36}$$

$\hat{\boldsymbol{K}}$ und $\hat{\boldsymbol{f}}$ now describe approximations of stiffness matrix $\boldsymbol{K}$ and force vector $\boldsymbol{f}$ of Eq. (36) due to the model reduction step. This leads to the approximate solution $\boldsymbol{d}_m$ of

$$\hat{\boldsymbol{K}}\boldsymbol{d}_m = \hat{\boldsymbol{f}}. \tag{37}$$

We want to find a relation between the residual $\boldsymbol{\rho} = \boldsymbol{f} - \boldsymbol{K}\boldsymbol{d}_m$ and the unknown error $\boldsymbol{e} = \boldsymbol{d} - \boldsymbol{d}_m$, as a small residual does not necessarily imply a small error. The

DWR approach is based on the assumption that in applications often only a certain functional of the solution is of interest: In fluid dynamics for example often not the complete velocity field around a body, but only its lift and drag coefficient have to be calculated with good accuracy, and in structural dynamics the engineer is often only interested in displacements or stresses at a certain point of the structure. This is then called a target functional $J(\boldsymbol{d})$ of the solution. The approximation yields a perturbed value $J(\boldsymbol{d}_m)$, and if we take for simplicity a linear functional, i.e.

$$J(\boldsymbol{d}) = \boldsymbol{p}^T \boldsymbol{d} \tag{38}$$

the error of the functional can be written as

$$J(\boldsymbol{d}) - J(\boldsymbol{d}_m) = J(\boldsymbol{e}) = \langle \boldsymbol{e}, \boldsymbol{p} \rangle. \tag{39}$$

Here $\langle \cdot, \cdot \rangle$ denotes a suitable inner product, in this case simply $\langle \boldsymbol{u}, \boldsymbol{v} \rangle = \boldsymbol{u}^T \boldsymbol{v}$.

If the functional is non-linear, we employ a Taylor expansion around the approximate solution and write

$$J(\boldsymbol{d}) - J(\boldsymbol{d}_m) = \left. \frac{\partial J(\boldsymbol{d})}{\partial \boldsymbol{d}} \right|_{\boldsymbol{d}_m} (\boldsymbol{d} - \boldsymbol{d}_m) + \text{h.o.t.} \tag{40}$$

Neglecting all terms of higher order and setting

$$\left. \frac{\partial J(\boldsymbol{d})}{\partial \boldsymbol{d}} \right|_{\boldsymbol{d}_m} \equiv \boldsymbol{p}^T, \tag{41}$$

we recover the same form as in Eq.(39), but with an "approximate" sign instead of the equality sign.

Now the DWR method introduces a second problem, the dual or adjoint problem,

$$\boldsymbol{K}^* \boldsymbol{\lambda} = \boldsymbol{p} \tag{42}$$

with $\boldsymbol{\lambda} \in \mathbb{R}^n$. The "external force" of the dual problem comes from the definiton of the functional $J(\boldsymbol{d})$. The dual operator $\boldsymbol{K}^*$ is defined via the Lagrange identity

$$\langle \boldsymbol{v}, \boldsymbol{K}\boldsymbol{u} \rangle = \langle \boldsymbol{K}^* \boldsymbol{v}, \boldsymbol{u} \rangle, \tag{43}$$

in our case we get $\boldsymbol{K}^* = \boldsymbol{K}^T$. Now we can write the error of the functional as

$$J(\boldsymbol{e}) = \langle \boldsymbol{e}, \boldsymbol{p} \rangle = \langle \boldsymbol{e}, \boldsymbol{K}^* \boldsymbol{\lambda} \rangle = \langle \boldsymbol{K}\boldsymbol{e}, \boldsymbol{\lambda} \rangle = \langle \boldsymbol{\rho}, \boldsymbol{\lambda} \rangle, \tag{44}$$

yielding the *a posteriori* error bound

$$|J(\boldsymbol{e})| \leq \sum_{i=1}^{n} |\rho_i| \, |\lambda_i| \tag{45}$$

with the local residual $\rho_i$, weighted with the local dual solution $\lambda_i$.

The dual problem of a non-linear system $\boldsymbol{F}(\boldsymbol{d}) = \boldsymbol{0}$ may be taken as the transpose of the mean value of the linearisation,

$$\overline{\boldsymbol{K}}^T \boldsymbol{\lambda} = \boldsymbol{p} \quad \text{with} \quad \overline{\boldsymbol{K}} = \int_0^1 \frac{\partial \boldsymbol{F}((1-s)\boldsymbol{d} + s\boldsymbol{d}_m)}{\partial \boldsymbol{d}} ds, \tag{46}$$

where the linearisation $\overline{\boldsymbol{K}}$ is evaluated between exact solution $\boldsymbol{d}$ and approximated solution $\boldsymbol{d}_m$. Then we obtain the identity, see [32],

$$\boldsymbol{F}(\boldsymbol{d}) - \boldsymbol{F}(\boldsymbol{d}_m) = \overline{\boldsymbol{K}}\ (\boldsymbol{d} - \boldsymbol{d}_m), \tag{47}$$

which is necessary for Eq.(44) to hold also for non-linear problems. But since the exact solution $\boldsymbol{d}$ is unkown, the matrix $\overline{\boldsymbol{K}}$ has to be evaluated at the approximate solution $\boldsymbol{d}_m$. This introduces an additional approximation error of the order $\|\boldsymbol{d} - \boldsymbol{d}_m\|^2$.

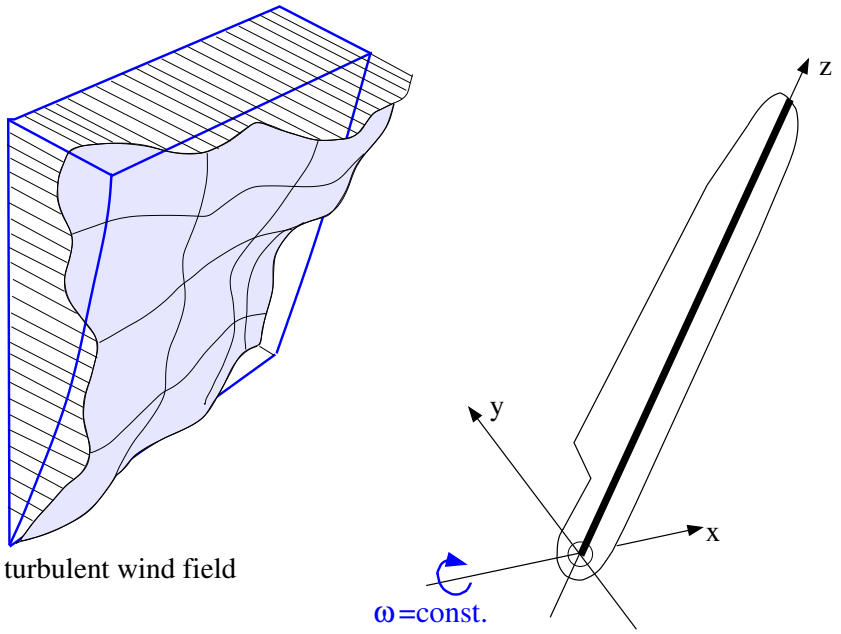


Figure 2: Model problem: Dynamics of a rotor blade in turbulent wind.

## 3.2 Application to Non-Linear Dynamics

The extension of the DWR method to the estimation of the model reduction error for non-linear dynamic problems as given by Eq.(1) with a non-linear functional

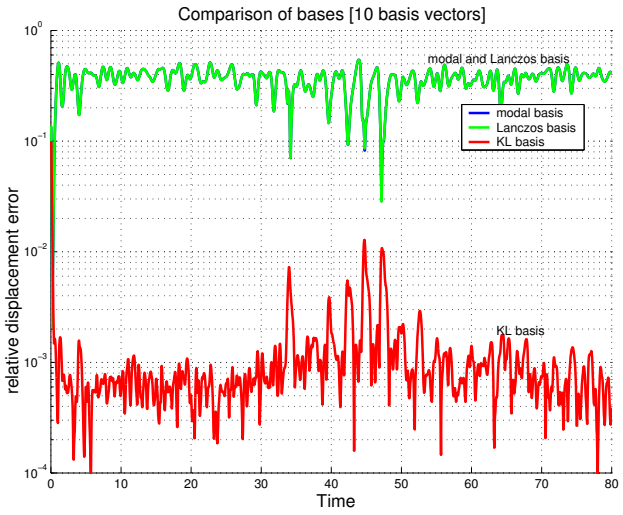


Figure 3: Time evolution of $e_{u,10}$ using $m = 10$ basis vectors. Modal and Lanczos basis yield the same approximation quality.

$J(\boldsymbol{d})$ is now simple. As shown in section 2, the model reduction process leads to the reduced model of the form

$$\boldsymbol{Y}_m^T \boldsymbol{F}(\boldsymbol{Y}_m \ddot{\boldsymbol{\xi}}, \boldsymbol{Y}_m \dot{\boldsymbol{\xi}}, \boldsymbol{Y}_m \boldsymbol{\xi}, t) = \boldsymbol{0}, \qquad t \in [0, T], \tag{48}$$

$$\boldsymbol{\xi}(0) = (\boldsymbol{Y}_m^T \boldsymbol{Y})^{-1} \boldsymbol{Y}_m^T \boldsymbol{d}_0, \tag{49}$$

$$\dot{\boldsymbol{\xi}}(0) = (\boldsymbol{Y}_m^T \boldsymbol{Y})^{-1} \boldsymbol{Y}_m^T \boldsymbol{v}_0, \tag{50}$$

with the residual

$$\boldsymbol{\rho}_m = \boldsymbol{F}(\boldsymbol{Y}_m \ddot{\boldsymbol{\xi}}, \boldsymbol{Y}_m \dot{\boldsymbol{\xi}}, \boldsymbol{Y}_m \boldsymbol{\xi}, t). \tag{51}$$

The dual problem for a non-linear dynamic problem is the linearisation of the original system along the approximated solution trajectory, for a derivation consult KLEIBER [26],

$$\boldsymbol{M}(t)^T \ddot{\boldsymbol{\lambda}} - \boldsymbol{C}(t)^T \dot{\boldsymbol{\lambda}} + \boldsymbol{K}(t)^T \boldsymbol{\lambda} = \boldsymbol{p}, \quad \boldsymbol{\lambda}(T) = \boldsymbol{0}, \quad \dot{\boldsymbol{\lambda}}(T) = \boldsymbol{0} \tag{52}$$

with

$$\boldsymbol{M}(t) = \left.\frac{\partial \boldsymbol{f}}{\partial \ddot{\boldsymbol{d}}}\right|_{\boldsymbol{d}_m}, \quad \boldsymbol{C}(t) = \left.\frac{\partial \boldsymbol{f}}{\partial \dot{\boldsymbol{d}}}\right|_{\boldsymbol{d}_m}, \quad \boldsymbol{K}(t) = \left.\frac{\partial \boldsymbol{f}}{\partial \boldsymbol{d}}\right|_{\boldsymbol{d}_m}. \tag{53}$$

Since these matrices have to be evaluated along the solution of the reduced problem, first one has to solve Eq.(48) for the time span $[0, T]$. Then the dual problem

has to be solved backwards in time, since end-point conditions are given. With the substitution $t = T - \tau$ the dual problem can be solved forward in time for $\tau$ and standard time integration algorithms can be used. With the dual solution $\boldsymbol{\lambda}$ and the residual $\boldsymbol{\rho}$ we can now express the error in the same way as in the linear case, as inner product of residual and dual solution,

$$J(\boldsymbol{d}) - J(\boldsymbol{d}_m) \approx \int_0^T \langle \boldsymbol{\lambda}, \boldsymbol{\rho} \rangle dt. \tag{54}$$

If the initial conditions are not equal to zero, the additional terms $\langle \boldsymbol{\lambda}(0), \boldsymbol{d}(0) - \boldsymbol{d}_m(0) \rangle$ and $\langle \dot{\boldsymbol{\lambda}}(0), \boldsymbol{v}(0) - \boldsymbol{v}_m(0) \rangle$ have to be added. Evaluating this approximation of the error can serve as a basis for resizing the reduced basis adaptively to obey a given error tolerance. Secondly, also the error due to the time discretisation is included in this estimate and can be used to adapt the time step.

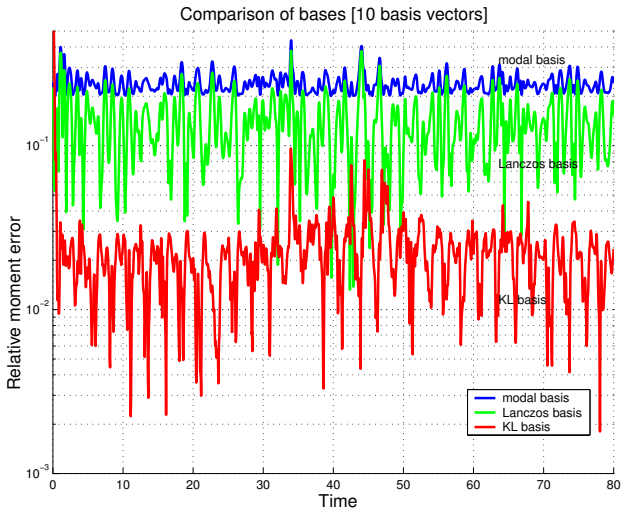


Figure 4: Time evolution of $e_{mb,10}$ using $m = 10$ basis vectors.

## 3.3 Choosing an Efficient Basis

Another possibility is to use the approximation of the error to choose only those basis vectors which are especially suited for the target functional: Starting from

$$J(\boldsymbol{d}) - J(\boldsymbol{d}_m) = \int_0^T \langle \boldsymbol{\rho}, \boldsymbol{\lambda} \rangle dt, \tag{55}$$

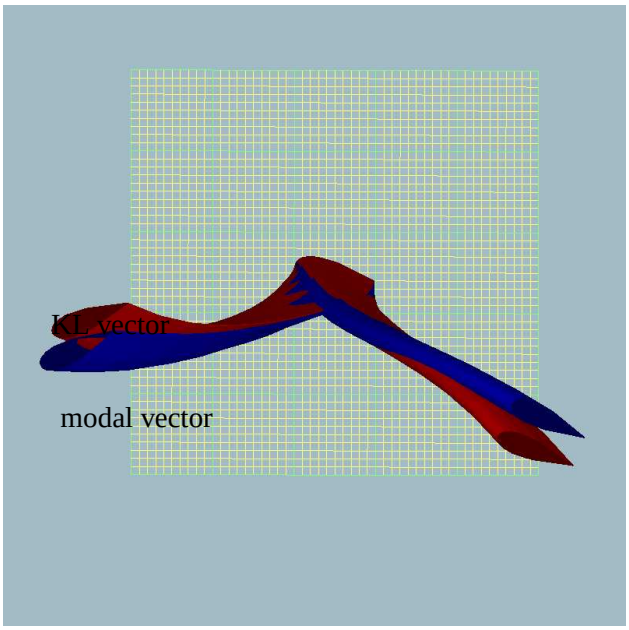


Figure 5: Superposition of second modal and KL vector

we write this equation as a sum of the individual components,

$$J(\boldsymbol{d}) - J(\boldsymbol{d}_m) = \sum_{i=1}^{n} r_i, \tag{56}$$

with vector $\boldsymbol{r} = (r_1, \ldots, r_d)^T$ defined by

$$\boldsymbol{r} = \int_0^T \boldsymbol{\Lambda}\boldsymbol{\rho}\, dt, \quad \boldsymbol{\Lambda} = \text{diag}(\boldsymbol{\lambda}). \tag{57}$$

If we project now on the subspace $\mathcal{V}_m$, we get

$$\boldsymbol{Y}_m^T \boldsymbol{r} = \int_0^T \boldsymbol{Y}_m^T \boldsymbol{\Lambda}\boldsymbol{\rho}\, dt, \tag{58}$$

where the individual components describe the amount of error along the corresponding basis vector. This approach is well established in adaptive mesh refinement. If the error component of an element is large, the element should be refined. In our case, elements correspond to basis vectors and those with large error components have to be kept in the reduced basis. On the other hand, if the error component is small, the basis vector can be rejected from the reduced basis. This reduces computational effort and yields the lowest-dimensional basis which is necessary to satisfy a given error tolerance of the target functional.

# 4 Numerical Examples

To demonstrate the applicability of the proposed model reduction approach we simulate the dynamic behaviour of the rotor blade of a modern wind turbine, as shown in Fig. 2. The rotor blade is discretised with beam elements as described in GERADIN and CARDONA [17]. These geometrically non-linear beam elements consider the rotational inertia of the beam's cross sections as well as the centrifugal and coriolis effects, thus both internal and inertial force vectors depend non-linearly on the nodal variables. The angular velocity of the rotor blade is kept constant at $\omega = 0.8\pi$ Hz and the blade is clamped at the blade root. The external forces are gravity loading and the aerodynamic loads due to a turbulent wind field. Thus we are faced with a non-linear system with additional aeroelastic effects. For all following simulations we employ the Newmark time integration method with $\beta = 1/4$ and $\gamma = 1/2$, a time step of $\Delta t = 0.05s$ and the Newton-Raphson method to solve the non-linear system of algebraic equations in each time step. How to efficiently solve the reduced model using this approach has been described in detail by KRYSL et al. [29].

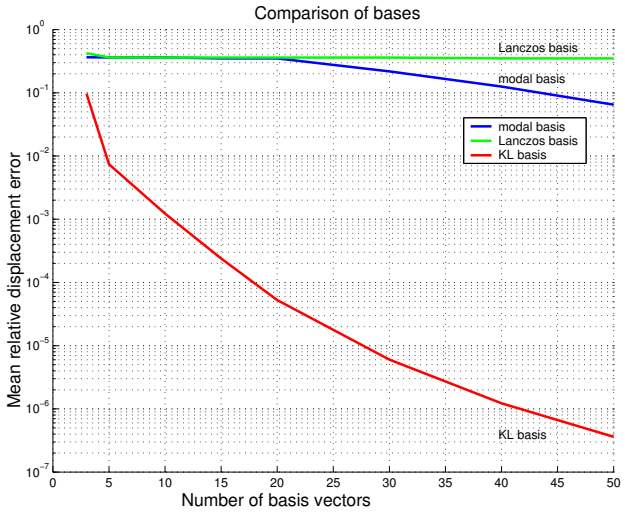


Figure 6: $E\{e_{u,m}\}$ over $m$ for modal, Lanczos and KL basis.

## 4.1 Comparison of the Bases

To compare the accuracy of different bases, we first calculate the modal, the Lanczos and the KL basis for the rotor blade. As initial conditions we use the solution

of the rotating system with a constant wind speed. The linearisation of the system, which is necessary for both the modal and the Lanczos basis, is evaluated at these initial conditions. In this way we incorporate centrifugal stiffening as well as the geometric non-linearity of the mean deflection in the calculation of the basis vectors. To obtain the KL basis we simulate two revolutions of the blade under turbulent wind loading. The snapshots thus include all geometric non-linearities and aeroelastic effects that did occur during these two revolutions.

We compare the accuracy of the three bases by simulating the dynamic behaviour of the rotor blade in turbulent wind for the time span $t \in [0 \dots 80]$ sec. To judge the quality of the approximated solutions we calculate the relative error of the displacements,

$$e_{u,m}(t) = \frac{\|\boldsymbol{u}_{\text{ref}} - \boldsymbol{u}_m\|}{\|\boldsymbol{u}_{\text{ref}}\|}, \tag{59}$$

as well as the relative error of the inner moments of the blade,

$$e_{mb,m}(t) = \frac{\|\boldsymbol{mb}_{\text{ref}} - \boldsymbol{mb}_m\|}{\|\boldsymbol{mb}_{\text{ref}}\|}. \tag{60}$$

Here the index $m$ denotes the size of the reduced basis. As exact solution $\boldsymbol{u}_{ref}$ und $\boldsymbol{mb}_{\text{ref}}$ we take the simulation result of the unreduced model.

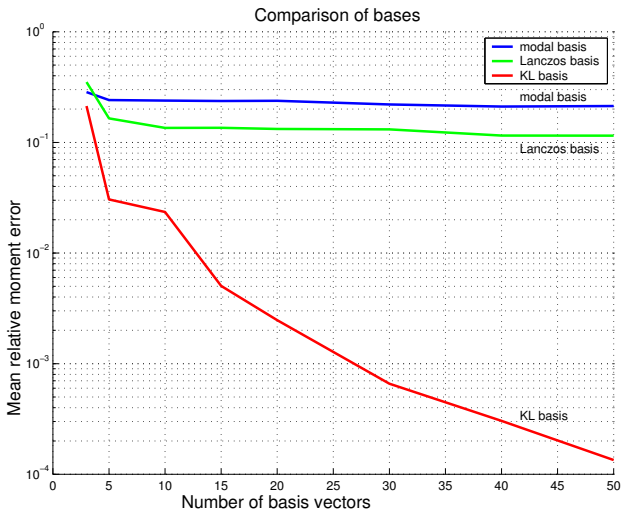


Figure 7: $E\{e_{mb,m}\}$ over $m$ for modal, Lanczos and KL basis.

In Figs. 3 and 4 we have depicted the time evolution of the relative error for the value $m = 10$. We see that in both pictures the KL basis yields a significantly

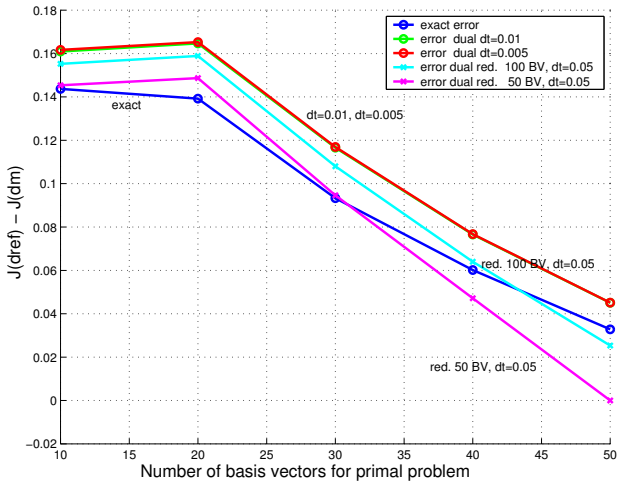


Figure 8: Comparsion of exact and estimated error

better approximation quality and that the Lanczos basis approximates the inner moments better than the modal basis. But due to the turbulent wind loading the results are not easy to compare. For the following investigations we will therefore compare the temporal mean values of the relative errors,

$$E(e_{u,m}) = \frac{1}{T}\int_0^T e_{u,m}(t)dt \quad \text{and} \quad E(e_{mb,m}) = \frac{1}{T}\int_0^T e_{mb,m}(t)dt. \tag{61}$$

In Fig. 6 the results for $E(e_{u,m})$, and in Fig. 7 the results for $E(e_{mb,m})$ are shown for modal, Lanczos and KL basis for $m = 3, 5, 10, 15, 20, 30, 40, 50$. Again we see the superior approximation quality of the KL basis: As the KL basis incorporates not only the non-linearities present during the time span used to obtain the snapshots, but also the aeroelastic effects, it yields such an improved approximation. These aeroelastic effects can be seen in Fig. 5, where the second vector of the modal and KL basis are superposed. This is called a lead-lag vector and describes a movement of the blade in the rotor plane: When the blade moves to the front, the aerodynamic lift will force it also upwards, and the KL basis clearly shows this behaviour, in contrast to the modal basis.

## 4.2 Employing the DWR Method

To approximate the error of a target functional with the DWR method, we have to solve the original problem forward and then the dual problem backwards in time. Since this is not feasible for the long time simulations of the wind turbine blade considered in this paper, we only employ the information gained in two

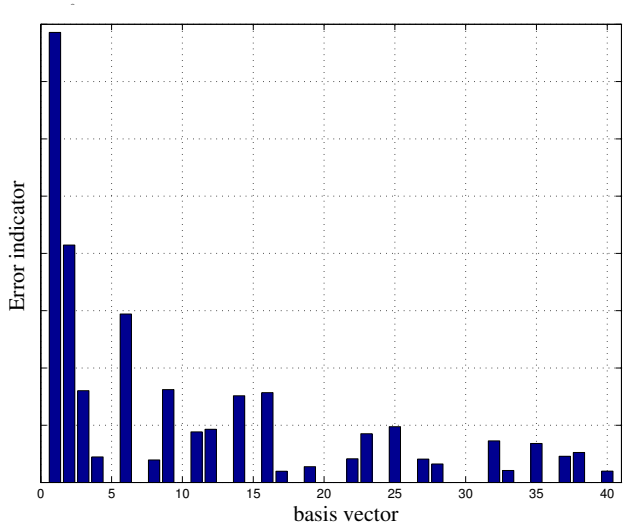


Figure 9: Error indicators for the modal basis

revolutions for the estimation of the error and the subsequent determination of an efficient low-dimensional basis. As functional we take the temporal mean of the tip displacement of the blade in the wind direction,

$$J(\boldsymbol{d}) = \int_0^T u_{x,tip}, \tag{62}$$

which is important when trying to detect collisions with the tower. We now solve the reduced problem forward in time and save the residual $\boldsymbol{\rho}$ and the approximated variables. Then we solve the dual problem for $\boldsymbol{\lambda}$ backwards in time and calculate the error estimate

$$J(\boldsymbol{d}_{ref}) - J(\boldsymbol{d}_m) \approx \int_0^T \boldsymbol{\lambda}^T \boldsymbol{\rho}\, dt. \tag{63}$$

In Fig. 8 we have depicted the results for the values $m_{primal} = 10, 20, \ldots 50$. The dual problem has been solved unreduced as well as reduced with $m_{dual} = 50, 100$ basis vectors. Also the influence of the time step length of the dual problem on the accuracy of the error estimate has been investigated. In all cases we see a good agreement of the estimated error with the exact error, which has been calculated using the results of the unreduced system. We also see the consequences of Galerkin orthogonality: If $m_{dual} \leq m_{primal}$, i.e. the dimension of the reduced dual prorblem is less or equal the dimension of the reduced original problem (and the same basis is used for both, as in our case), the solution $\boldsymbol{\lambda}_m$ is orthogonal to the residual $\boldsymbol{\rho}_m$ and no information about the error can be gained.

Finally we show the appicability of the proposed indicator for the importance of the individual basis vectors for the target functional: For each of the basis vectors used for the reduced model we can calculate the product of residual and dual solution, integrate this over time to obtain a value for the indicator, as depicted in Fig. 9 for the modal basis. Those vectors with large values are more important for the accuracy of the solution and have to be kept in the basis. If the eigenvectors are orderd according to their indicator value, we can compare the approximation quality of this improved basis with a basis, where the criterium has been the frequency (modal basis) or the energy content (KL basis). In Figs. 10 and 11 we have compared the relative error of the functional using the normal and the improved basis. We see in both cases a significant improvement of the approximation quality, when using the basis that has been specially designed for the target functional of interest.

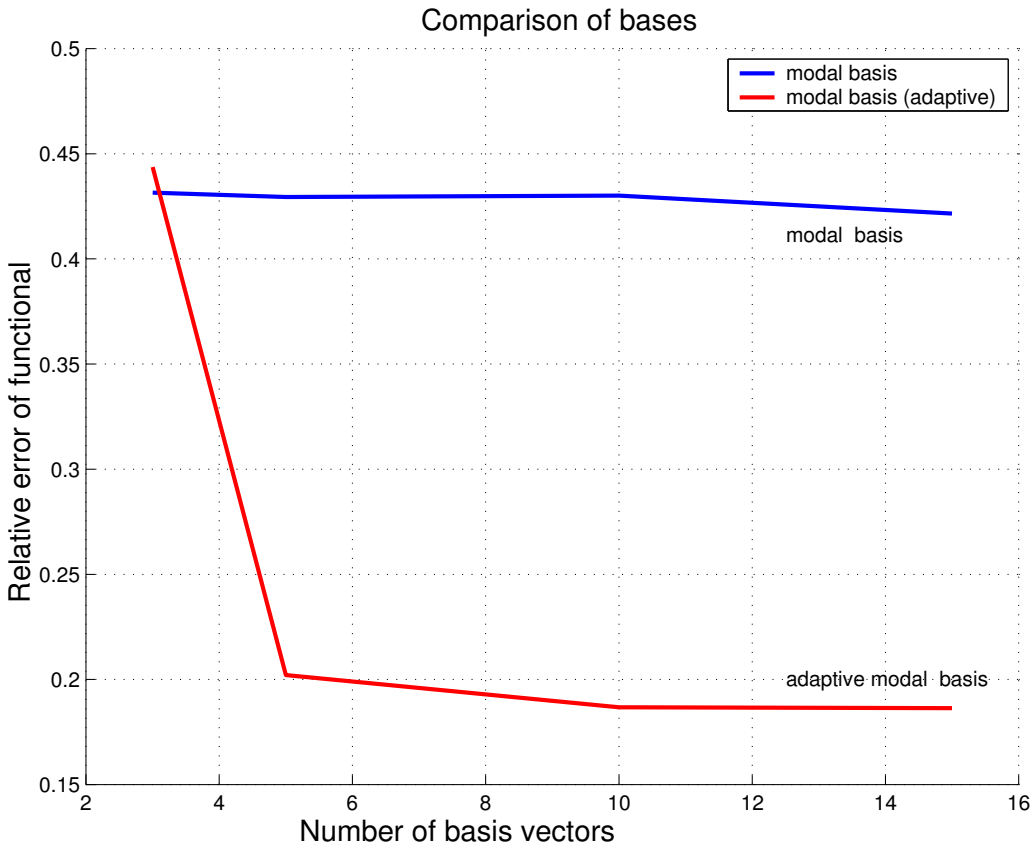


Figure 10: Relative error of $J$ over $m$ for the modal basis

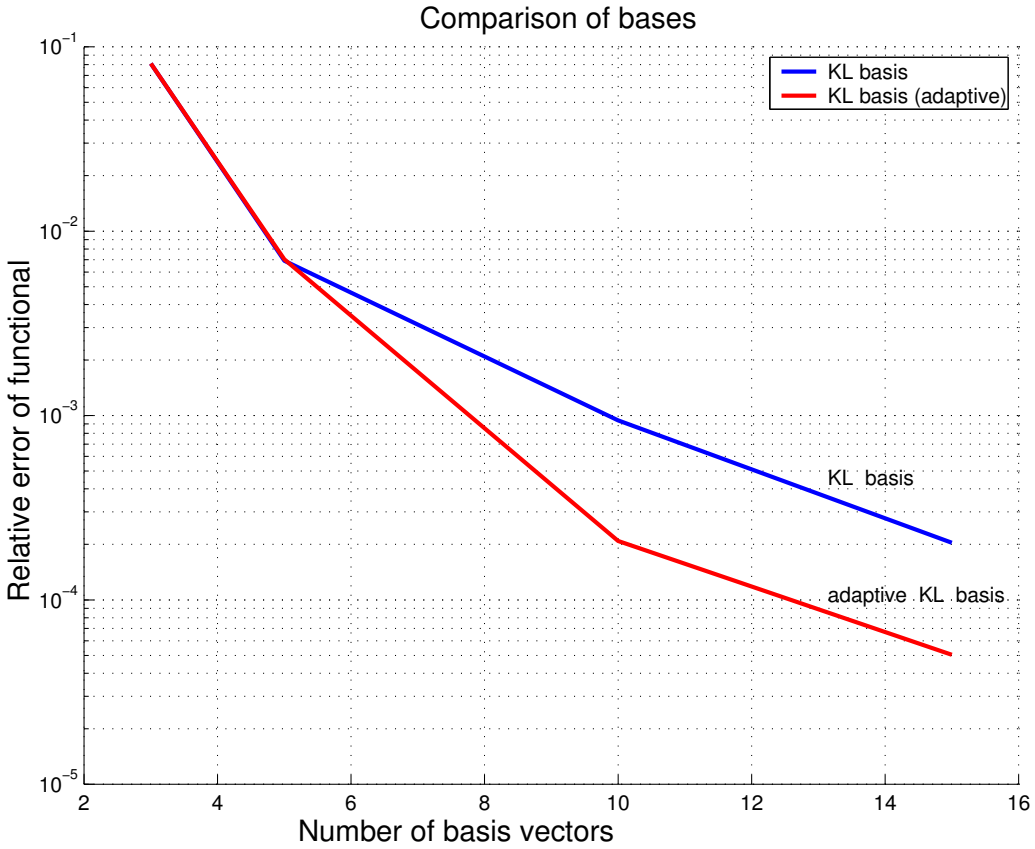


Figure 11: Relative error of $J$ over $m$ for the KL basis

# 5 Conclusions

The projection-based model reduction was employed on a nonlinear structural model of a horizontal axis wind turbine rotor blade as to be able to perform long time integrations with as few degrees of freedom as possible while at the same time the induced error is under direct control. Three different choices for the reduced basis, the modal basis, the Lanczos basis and the Karhunen-Loève basis, have been compared. It has been shown that the Karhunen-Loève basis is far more accurate than the other bases due to the automatic incorporation of nonlinear and aeroelastic effects. Furthermore the error induced by the model reduction step has been analysed incorporating the dual-weighted-residual method. Using this method it is possible to obtain an à priori error estimate for a certain target functional of the solution. This error estimate can be used for adaptively resizing the number of basis vectors and the length of the time step to satisfy a given

error tolerance. It can also be used to form a very efficient low-dimensional basis especially tailored to the target functional of interest. In our computations this basis yields a significantly better approximation of the functional when compared to conventionally choosen bases.

# References


[1] B.O. Almroth, P. Stern, and F.A. Brogan. Automatic choice of global shape functions in structural analysis. *AIAA Journal*, 16(5):525–528, 1978.

[2] W. Bangert and R. Rannacher. Finite element approximation of the acoustic wave equation: Error control and mesh adaptation. *East-West Journal of Numerical Mathematics*, 7(4):263–282, 1999.

[3] O. Baysal and M.E. Eleshaky. Aerodynamic sensitivity analysis methods for the compressible Euler equations. *Journal of Fluids Engineering*, 113:681–688, 1991.

[4] R. Becker and R. Rannacher. A feed-back approach to error control in finite element methods: Basic analysis and examples. *East-West Journal for Numerical Mathematics*, 4:237–264, 1996.

[5] R. Becker and R. Rannacher. Weighted a posteriori error control in finite element methods. Technical report, Universität Heidelberg, 1996.

[6] R. Becker and R. Rannacher. An optimal control approach to a posteriori error estimation in finite elements. *Acta Numerica*, 10:1–102, 2001.

[7] G. Berkooz, P. Holmes, and J.L. Lumley. The proper orthogonal decomposition in the analysis of turbulent flows. *Annual Reviews of Fluid Mechanics*, 25:539–575, 1993.

[8] C. Bucher. Stabilization of explicit time integration by modal reduction. In W.A. Wall, K.U. Bletzinger, and K. Schweizerhof, editors, *Trends in Computational Structural Mechanics*, Barcelona, 2001. CIMNE.

[9] C. Cabos. Error bounds for dynamic responses in forced vibration problems. *SIAM Journal of Scientific Computing*, 15(1):1–15, 1994.

[10] D. Dinkler. Reduction methods in structural dynamics. In K. Meskouris and U. Wittek, editors, *Aspects in Modern Computational Structural Analysis*, pages 19–31. Balkema, 1997.

[11] K. Eriksson, D. Estep, P. Hansbo, and C. Johnson. Introduction to adaptive methods for differential equations. *Acta Numerica*, 4:105–158, 1995.

[12] K. Eriksson, D. Estep, P. Hansbo, and C. Johnson. *Computational Differential Equations*. Cambridge University Press, Cambridge, 1996.

[13] D. Estep. A posteriori error bounds and global error control for approximations of ordinary differential equations. *SIAM Journal of Numerical Analysis*, 32:1–48, 1995.

[14] J.P. Fink and W.C. Rheinboldt. On the discretization error of parametrized nonlinear equations. *SIAM Journal of Numerical Analysis*, 20(4):732–746, 1983.

[15] J.P. Fink and W.C. Rheinboldt. On the error behaviour of the reduced basis technique for nonlinear finite element approximations. *ZAMM*, 63:21–28, 1983.

[16] G.H. Golub and C.F. van Loan. *Matrix Computations, 3rd Ed.* Johns Hopkins University Press, Baltimore, 1996.

[17] M Géradin and A. Cardona. *Flexible Multibody Dynamics, A Finite Element Approach*. John Wiley & Sons, Chichester, 2001.

[18] H. Harman. *Modern Factor Analysis*. University of Chicago Press, Chicago, 1960.

[19] P. Holmes, J.L. Lumley, and G. Berkooz. *Turbulence, Coherent Structures, Dynamical Systems and Symmetry*. Cambridge University Press, Cambridge, 1996.

[20] H. Hotelling. Analysis of complex statistical variables in principal components. *Journal of Experimental Psychology*, 24:417, 1953.

[21] S.R. Idelson and A. Cardona. A reduction method for nonlinear structural dynamic analysis. *Computer Methods in Applied Mechanics and Engineering*, 49:253–279, 1985.

[22] A. Jameson. Aerodynamic design via control theory. *SIAM Journal of Scientific Computing*, 3:233–260, 1988.

[23] C. Johnson. Error estimates and adaptive time-step control for a class of one-step methods for stiff ordinary differential equations. *SIAM Journal of Numerical Analysis*, 25(4):908–926, 1988.

[24] K.J. Joo, E.L. Wilson, and P. Leger. Ritz vectors and generation criteria for mode superposition analysis. *Earthquake Engineering and Structural Dynamics*, 18:149–167, 1989.

[25] K. Karhunen. Zur Spektraltheorie stochastischer Prozesse. *Annales Academiae Scientarum Fennicae*, 37, 1946.

[26] M. Kleiber. *Parameter Sensitivity in Nonlinear Mechanics*. John Wiley & Sons, Chichester, 1997.

[27] K.A. Kline. Dynamic analysis using a reduced basis of exact modes and Ritz vectors. *AIAA Journal*, 24(12):2022–2029, 1986.

[28] E. Kreuzer and O. Kust. Analysis of long torsional springs by proper orthogonal decomposition. *Archive of Applied Mechanics*, 67:68–80, 1996.

[29] P. Krysl, S. Lall, and J.E. Marsden. Dimensional model reduction in nonlinear finite element dynamics of solids and structures. *International Journal for Numerical Methods in Engineering*, 51:479–504, 2001.

[30] P. Leger and S. Dussault. Non-linear seismic response analysis using vector superposition methods. *Earthquake Engineering and Structural Dynamics*, 21:163–176, 1992.

[31] A. Logg. Multi-adaptive error control for ODEs. Preprint 2000-003, Chalmers Finite Element Center, 2000.

[32] A. Logg. A multiadaptive ODE-solver. Preprint 2000-002, Chalmers Finite Element Center, 2000.

[33] E.N. Lorenz. Empirical orthogonal eigenfunctions and statistical weather prediction. Technical report, MIT Report, Department of Meteorology, Cambridge, MA, 1956.

[34] M.M. Loève. *Probability Theory*. Van Nostrand, New Jersey, 1955.

[35] J.L. Lumley. The structure of inhomogeneous turbulent flows. In A.M. Yaglom and V.I. Tatarski, editors, *Atmospheric Turbulence and Radio Wave Propagation*, 1967.

[36] G.I. Marchuk. *Adjoint Equations and Analysis of Complex Systems*. Kluwer Academic Publishers, Dordrecht, 1995.

[37] R.E. Nickell. Nonlinear dynamics by mode superposition. *Computer Methods in Applied Mechanics and Engineering*, 7:107–129, 1976.

[38] A.K. Noor. Recent advances and applications of reduction methods. *Appl. Mech. Rev.*, 47(5):125–145, 1994.

[39] A.K. Noor and J.M. Peters. Reduced basis technique for nonlinear analysis of structures. *AIAA Journal*, 18(4):455–462, 1980.

[40] B. Nour-Omid and R.W. Clough. Dynamic analysis of structures using Lanczos co-ordinates. *Earthquake Engineering and Structural Dynamics*, 12:565–577, 1984.

[41] R. Rannacher. The dual-weighted-residual method for error control and mesh adaptation in finite element methods. In J.R. Whiteman, editor, *MAFE-LEAP 99*, pages 97–115, Amsterdam, 2000. Elsevier.

[42] R. Rannacher and C. Johnson. On error control in computational fluid mechanics. Technical report 94-13, Universität Heidelberg, 1994.

[43] J. Remke and H. Rothert. Eine modale Reduktionsmethode zur geometrisch nichtlinearen statischen und dynamischen Finite-Element-Berechnung. *Archive of Applied Mechanics*, 63:101–115, 1993.

[44] Y. Saad. *Numerical Methods for Large Eigenvalue Problems*. Manchester University Press, Manchester, 1992.

[45] C. Sansour, P. Wriggers, and J. Sansour. Time integration and reduction methods in nonlinear dynamics of solids. In *GAMM 2001, Zürich*, 2001.

[46] L. Sirovitch. Turbulence and the dynamics of coherent structures, Part I-II. *Quarterly of Applied Mathematics*, 45:561–590, 1987.

[47] L Sirovitch and R. Everson. Management and analysis of large scientific datasets. *International Journal of Supercomputer Applications*, 6(1):50–68, 1992.

[48] S. Utku, L.M. Clemente, and S. Moktar. Errors in reduction methods. *Computers and Structures*, 21(6):1153–1157, 1985.

[49] E.L. Wilson, M. Yuan, and J.M. Dickens. Dynamic analysis by direct superposition of Ritz vectors. *Earthquake Engineering and Structural Dynamics*, 10:813–821, 1982.

[50] P. Wriggers. *Nichtlineare Finite-Element-Methoden*. Springer Verlag, Berlin, 2001.

Technische Universität Braunschweig
Informatik-Berichte ab Nr. 1998-04

| | | |
|---|---|---|
| 1998-04 | C. Lindig | Analyse von Softwarevarianten |
| 1998-05 | Gregor Snelting, Frank Tip | Reengineering Class Hierarchies Using Concept Analysis |
| 1998-06 | Juliana Küster Filipe | On a Distributed Temporal Logic for Modular Object Systems |
| 1998-07 | J. Schönwälder, M. Bolz, S. Mertens, J. Quittek, A. Kind, J. Nicklisch | SMX - Script MIB Extensibility Protocol Version 1.0 |
| 1998-08 | C. Heimann, S. Lauterbach, T. Förster | Entwurf und Implementierung eines verteilten Ansatzes zur Lösung langrechnender Optimierungsprobleme aus dem Bereich der Ingenieurwissenschaften |
| 1999-01 | A. Zeller | Yesterday, my program worked. Today, it does not. Why? |
| 1999-02 | P. Niebert | A Temporal Logic for the Specification and Verification of Distributed Behaviour |
| 1999-03 | S. Eckstein, K. Neumann | Konzeptioneller Entwurf mit der Unified Modeling Language |
| 1999-04 | T. Gehrke, A. Rensink | A Mobile Calculus with Data |
| 2000-01 | T. Kaiser, B. Fischer, W. Struckmann | The Modula-2 Proving System MOPS |
| 2000-02 | J. Saperia, J. Schönwälder | Policy-Based Enhancements to the SNMP Framework |
| 2000-03 | A. Casties | Finite-Element-Interpolation der rumlichen Dichten eines Vielteilchensystems auf ungeordneten Gittern |
| 2000-04 | J. Koslowski | A 2-dimensional view of the Chu-construction |
| 2000-05 | S. Eckstein, P. Ahlbrecht, K. Neumann | Von parametrisierten Spezifikationen zu generierten Informationssystemen: ein Anwendungsbeispiel |
| 2000-06 | F. Strauß, J. Schönwälder, M. Mertens | JAX - A Java AgentX Sub-Agent Toolkit |
| 2000-07 | F. Strauß | Advantages and Disadvantages of the Script MIB Infrastructure |
| 2000-08 | T. Gehrke, U. Goltz | High-Level Sequence Charts with Data Manipulation |
| 2000-09 | T. Firley | Regular languages as states for an abstract automaton |
| 2001-01 | K. Diethers | Tool-Based Analysis of Timed Sequence Diagrams |
| 2002-01 | R. van Glabbeek, U. Goltz | Well-behaved Flow Event Structures for Parallel Composition and Action Refinement |
| 2002-02 | J. Weimar | Translations of Cellular Automata for Efficient Simulation |
| 2002-03 | H. G. Matthies, M. Meyer | Nonlinear Galerkin Methods for the Model Reduction of Nonlinear Dynamical Systems |
| 2002-04 | H. G. Matthies, J. Steindorf | Partitioned Strong Coupling Algorithms for Fluid-Structure-Interaction |
| 2002-05 | H. G. Matthies, J. Steindorf | Partitioned but Strongly Coupled Iteration Schemes for Nonlinear Fluid-Structure Interaction |
| 2002-06 | H. G. Matthies, J. Steindorf | Strong Coupling Methods |
| 2002-07 | H. Firley, U. Goltz | Property Preserving Abstraction for Software Verification |
| 2003-01 | M. Meyer, H. G. Matthies | Efficient Model Reduction in Non-linear Dynamics Using the Karhunen-Loève Expansion and Dual-Weighted-Residual Methods |